

Apatite formation of bioactive glasses is enhanced by low additions of fluoride but delayed in the presence of serum proteins

Furqan A. Shah^{a,*}, Delia S. Brauer^{b,#}, Robert G. Hill^b, Karin A. Hing^a

^aSchool of Engineering and Materials Science, ^bDental Physical Sciences, Barts and the London School of Medicine and Dentistry, Queen Mary University of London, Mile End Road, London, E1 4NS, UK.

*Corresponding author: Present address: Department of Biomaterials, Sahlgrenska Academy at University of Gothenburg, Box 412, 405 30, Göteborg, Sweden, *Tel.*: +46 (0) 31 786 28 98; *E-mail*: furqan.ali.shah@biomaterials.gu.se

[#]Present address: Otto-Schott-Institut, Friedrich-Schiller-Universität, Fraunhoferstr. 6, 07743 Jena, Germany

Abstract

Five bioactive glass compositions in the $\text{SiO}_2\text{-P}_2\text{O}_5\text{-CaO-Na}_2\text{O-CaF}_2$ system (0 – 32 mol% CaF_2) and Bioglass® 45S5 were evaluated for their apatite forming ability in serum-free and serum-containing cell culture media for up to seven days. While F^- ions in low concentrations were found to enhance apatite formation, higher fluoride content caused formation of fluorite and calcite. The presence of serum proteins delayed apatite precipitation for all compositions, while Bioglass® 45S5, despite considerably higher phosphate content (2.6 vs. ≤ 1.1 mol% P_2O_5) and high concentrations of Ca^{2+} and PO_4^{3-} in solution, formed only amorphous calcium phosphate.

Highlights

- Low concentrations of fluoride enhance apatite formation in bioactive glasses
- Serum proteins retard apatite precipitation with minimal effect on ion release
- Ion concentrations remain high at later time points in serum-containing media as a consequence of reduced apatite formation

Keywords

bioactive glass, serum proteins, in vitro, fluorapatite, cell culture medium

1. Introduction

Bioactive glass (BG) is known to bond to hard and soft tissues [1]. Fluoride-containing glasses are of particular interest owing to their ability to form fluorapatite, which exhibits better chemical stability than fluoride-free apatites [2]. Fluoride has well documented antibacterial properties [3], and in low concentrations fluoride ions increase bone mass and mineral density [4]. Furthermore, fluoride-containing bioactive glasses enhance osteoblast proliferation, differentiation and mineralization [5].

Novel BG compositions are evaluated in vitro for their apatite forming ability in physiologically relevant test solutions such as SBF [6], Tris-buffer solutions [7], and cell culture media [8].

Dissolution and precipitation forms an amorphous calcium phosphate surface layer in the early reaction stages [9], which later undergoes crystallization to apatite by CO_3^{2-} , OH^- , and/or F^- anion incorporation. This surface apatite is able to elicit an interfacial biological response, resulting in bond formation between tissues and the synthetic material, i.e., bioactive fixation [10]. However, pivotal to this bioactivity is controlling the release rates of ionic dissolution products, i.e., Ca^{2+} and Si^{4+} ions [11]. Dissolution kinetics and consequently the rate of apatite formation is directly related to atomic structure [12], which therefore are critical to in vivo performance.

Although in vivo conditions do not parallel simulated in vitro conditions [13], certain proteins induce specific biological effects in simulated model systems [14]. Amino acids [15], proteins [16], and other organic molecules are rapidly adsorbed onto the glass surface and interfere with apatite formation and

stability of the precipitated surface layers. The present work investigates the role of serum proteins in attenuating the in vitro apatite forming ability of fluoride-containing bioactive glasses.

2. Materials and Methods

Five BG compositions in the $\text{SiO}_2\text{-P}_2\text{O}_5\text{-CaO-Na}_2\text{O-CaF}_2$ system were prepared by conventional melt-quench route as described earlier [8, 17]. Bioglass® 45S5 was prepared as control (**Table I**). Glass powders were immersed in two dissolution media based on Eagle's Minimal Essential Medium with Earle's Salts (MEM). Briefly, both media contained 2.2 g/L NaHCO_3 , 20 mL/L HEPES buffer solution, and were nominally Si^{4+} and F^- free; HC-MEM (pH=7.4) was serum-free, while HS-MEM (pH=7.3) contained 10% of heat-inactivated foetal bovine serum (Sigma-Aldrich) as described previously [8, 18]. Dissolution experiments, elemental analysis, characterization of glass powders by FTIR and XRD were performed as described previously [8].

One-way analysis of variance (ANOVA) with *post hoc* Bonferroni analysis (SPSS Statistics, v.20, IBM Corp.) was used for statistical analysis; p values < 0.05 were considered statistically significant. Mean values \pm standard deviations are presented.

Table I: Nominal glass compositions (mol%)

Glass	SiO_2	P_2O_5	CaO	Na_2O	CaF_2	Classification
Bioglass® 45S5	46.1	2.6	26.9	24.4	-	fluoride-free
F0	49.47	1.07	23.08	26.38	-	
F4	47.12	1.02	21.98	25.13	4.75	low-fluoride
F9	44.88	0.97	20.94	23.93	9.28	
F17	40.68	0.88	18.98	21.69	17.76	high-fluoride
F32	33.29	0.72	15.53	17.75	32.71	

3. Results and Discussion

Glass dissolution, by ion exchange and dissolution of the silicate network through a combination of Si-O-Si bond breakage [19] and silicate chain dissolution [20], caused a rapid increase in Ca^{2+} , Si^{4+} and F^- concentrations between days 0 and 3. Conversely, P (or PO_4^{3-}) depletion closely mirrored apatite formation. On day 3, concentrations of Ca^{2+} and PO_4^{3-} were generally higher in the serum-containing medium, HS-MEM (**Figure 1**). Between days 3 and 7, Ca^{2+} and Si^{4+} (not shown) concentrations decreased slightly, and F^- concentrations remained approximately constant. PO_4^{3-} concentrations decreased in both solutions; however, the decrease was much more pronounced in HC-MEM, coinciding with faster apatite formation.

On day 7, ionic concentrations were also generally higher in the serum-containing HS-MEM medium, with differences in Ca^{2+} and F^- being less pronounced for low-fluoride glasses (F4 and F9).

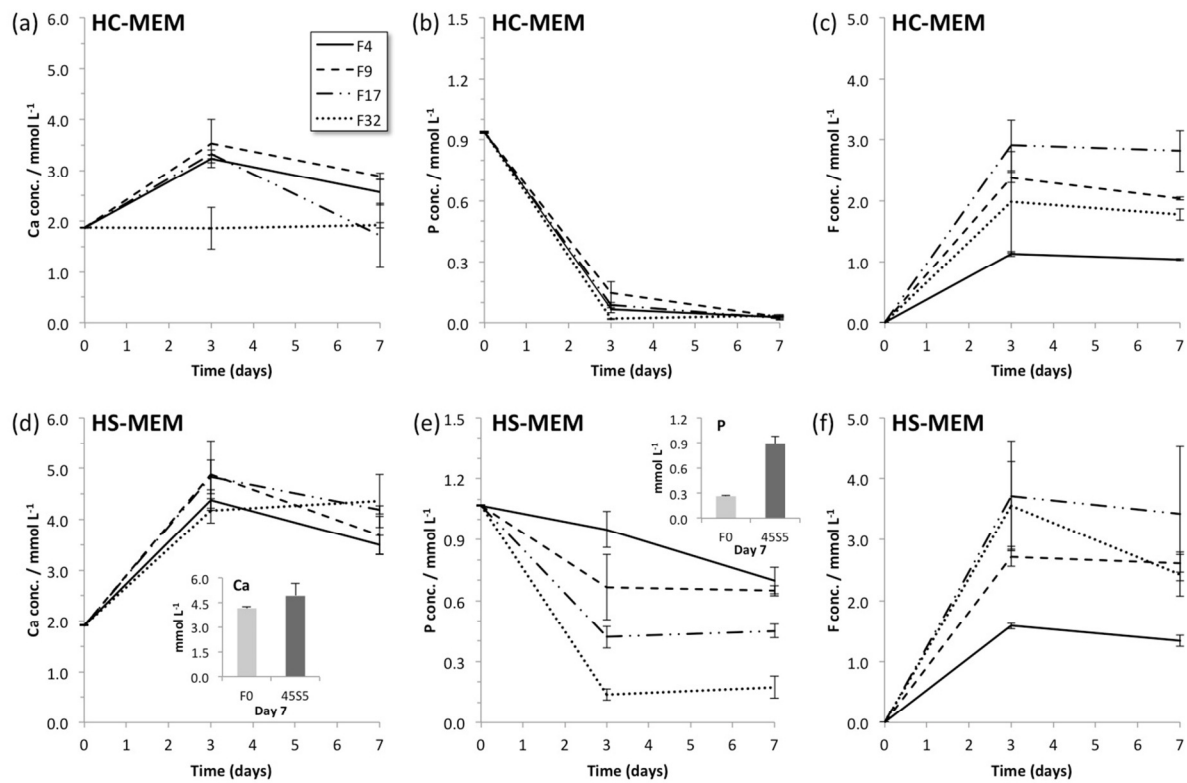


(Figure 1)

At day 7, 45S5 (insets in **Figure 1**) serum containing media showed higher Ca²⁺ and PO₄³⁻ concentrations than those of all other glasses, with the significantly higher phosphate concentration most likely to be due to an absence of apatite formation, and thus of PO₄³⁻ sequestering from solution. The Ca²⁺ concentration for F0 was comparable to all fluoride-containing glasses, while PO₄³⁻ concentration for F0 was lower than all fluoride-containing glasses (except F32).

FTIR (**Figure 2**) and XRD (**Figure 3**) showed changes after BG immersion. In serum-free conditions (HC-MEM), apatite was detected as early as day 3 for the low-fluoride glasses. In the presence of serum (HS-MEM), apatite formation was delayed and could be detected for the low-fluoride glasses at 7 days, while glass F17 only formed amorphous calcium phosphate (broad absorption band at 566 cm⁻¹). Owing to its high fluoride content, F32 only showed high intensity Bragg peaks corresponding to fluorite (CaF₂) formation in both media.

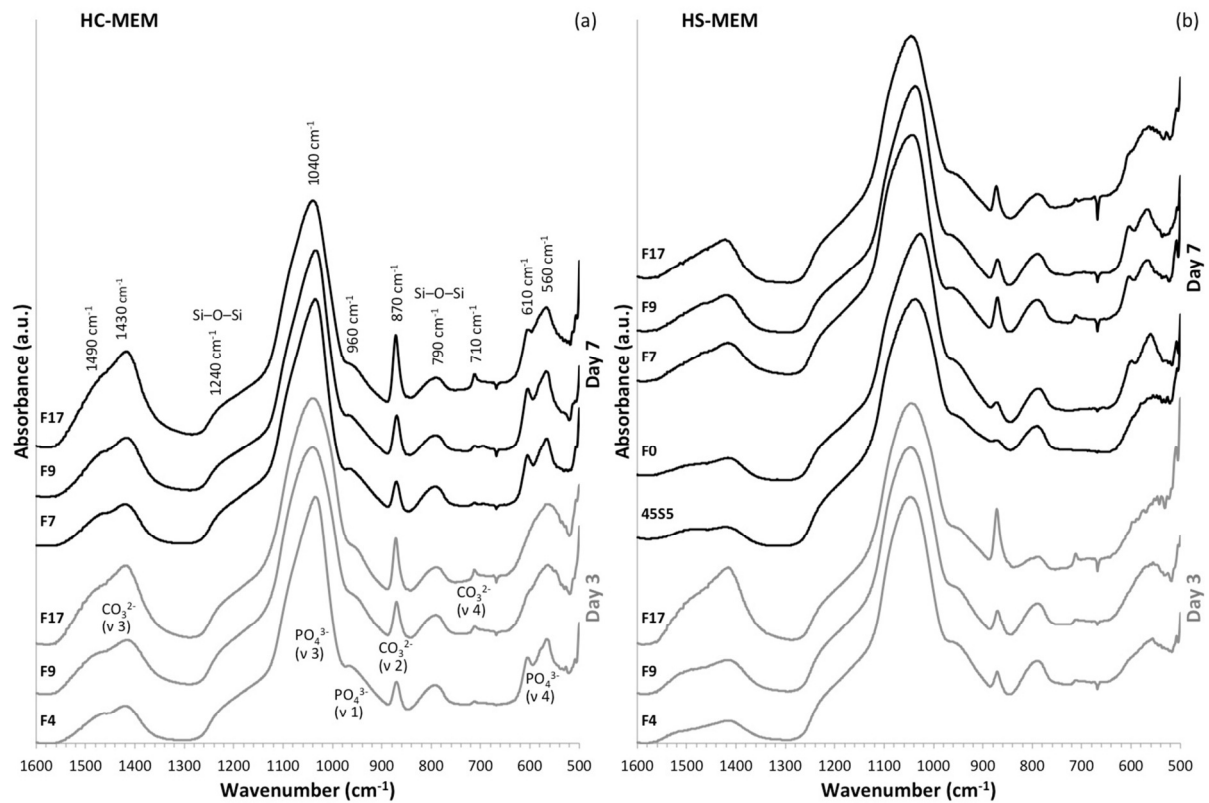


(Figure 2)

Apatite formation increased with reaction time. For the fluoride-containing glasses, FTIR bands for PO_4^{3-} at 1040 cm^{-1} became sharper while the $560\text{--}610\text{ cm}^{-1}$ domain resolved into two well-defined bands. These are characteristic of crystalline calcium orthophosphates including apatite. XRD showed presence of apatite-specific reflections and a shift in the position of the amorphous halo to lower 2θ -values compared to the unreacted glasses [21], representing the ion-depleted glass. Apatite was also detected for F0 at 7 days of immersion in HS-MEM, while 45S5 showed an amorphous halo in XRD and a single broad absorption band at 566 cm^{-1} in FTIR, suggesting amorphous calcium phosphate or poorly crystalline apatite.

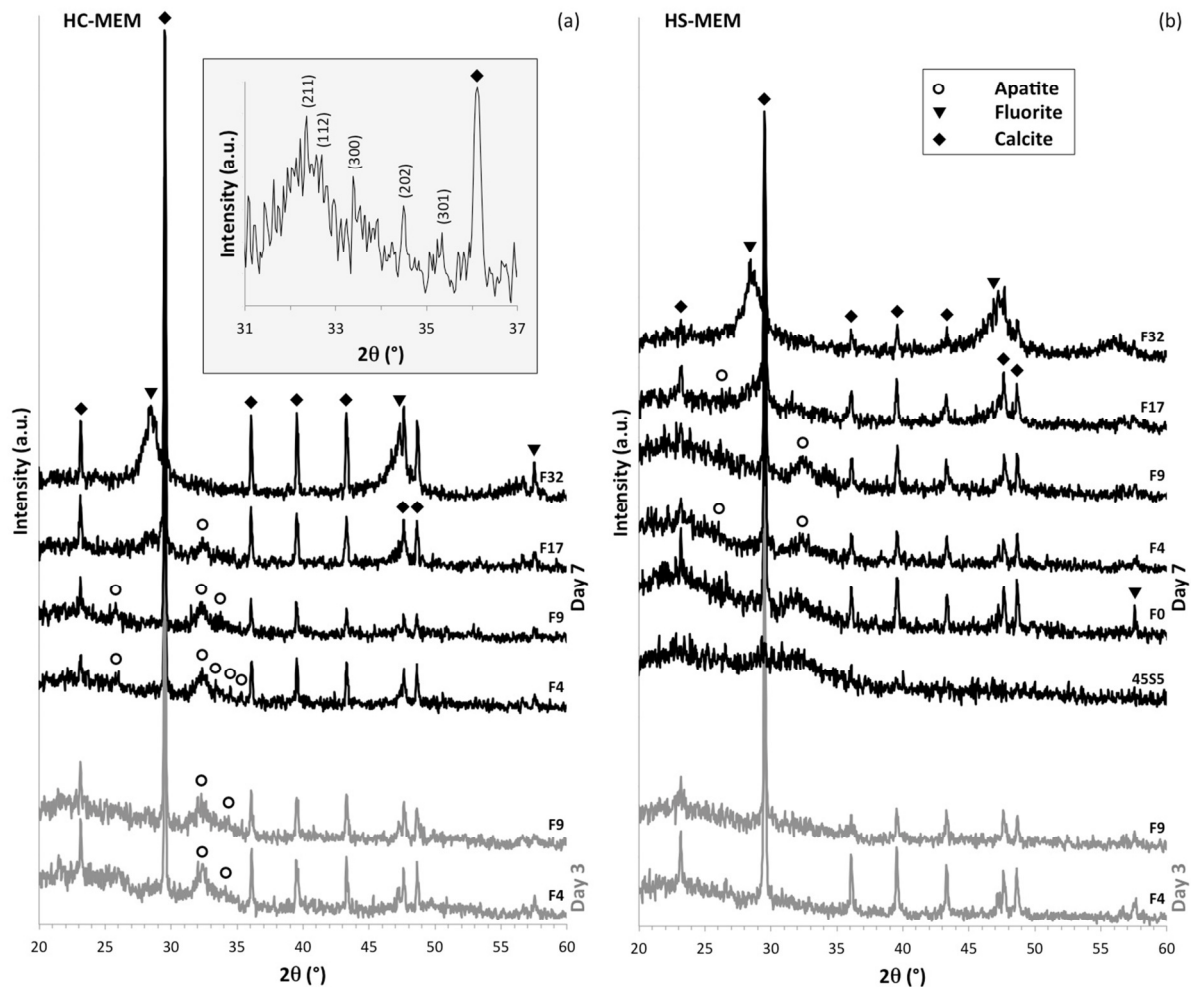


(Figure 3)

FTIR bands for CO_3^{2-} at 710, 870 and $1400\text{--}1500\text{ cm}^{-1}$ indicated carbonate incorporation into the apatite. Only B-type CO_3^{2-} substitutions are believed to occur in test solutions containing $\text{HCO}_3^- \leq 20\text{ mmol L}^{-1}$ [22]. However, both HC- and HS- media contain $\approx 26\text{ mmol L}^{-1}\text{ HCO}_3^-$, and therefore the possibility of A-type substitutions exists. Indeed, the vibration at 1480 cm^{-1} has been attributed to a “minor A-type” CO_3^{2-} -substitution [23].

The Ca:P (mol%) ratio increased with increasing CaF_2 content. It is apparent that this Ca (but also fluoride) excess results in the formation of additional calcium-containing phases, i.e. calcite and fluorite. In contrast to previous experiments conducted using nominally carbonate-free media [17], all XRD patterns (except 45S5) were dominated by high intensity peaks associated with calcite, which increased in intensity with increasing calcium content. The limited availability of PO_4^{3-} influenced the relative quantities of the different crystalline phases, particularly with respect to the amount of F^- ions being incorporated into either fluorapatite or fluorite. Therefore following PO_4^{3-} depletion, HCO_3^- ions in solution and remaining Ca^{2+} ions form calcite, while excess F^- and Ca^{2+} ions form fluorite.

4. Conclusions

Fluoride ions in low concentrations were clearly beneficial for apatite formation of BG, while higher fluoride content resulted in formation of fluorite and calcite. The presence of serum proteins delayed apatite precipitation for fluoride-containing glasses, while Bioglass® 45S5, despite a considerably higher phosphate content, formed only amorphous calcium phosphate.

Acknowledgements

The authors thank Drs. RM Wilson, ZB Luklinska, and AJ Parish for assistance with XRD and SEM; and NRM Laboratory, UK, for the ICP-OES analyses. Financial support from QMUL International Science and Excellence Award is gratefully acknowledged.

References

- [1] Hench LL, Polak JM. Third-Generation Biomedical Materials. *Science*. 2002;295:1014-7.
- [2] Aoba T. The Effect of Fluoride On Apatite Structure and Growth. *Crit Rev Oral Biol Med*. 1997;8:136-53.
- [3] Lindfors NC, Hyvonen P, Nyssonen M, Kirjavainen M, Kankare J, Gullichsen E, et al. Bioactive glass S53P4 as bone graft substitute in treatment of osteomyelitis. *Bone*. 2010;47:212-8.
- [4] Vestergaard P, Jorgensen N, Schwarz P, Mosekilde L. Effects of treatment with fluoride on bone mineral density and fracture risk - a meta-analysis. *Osteoporos Int*. 2008;19:257-68.
- [5] Gentleman E, Stevens MM, Hill RG, Brauer DS. Surface properties and ion release from fluoride-containing bioactive glasses promote osteoblast differentiation and mineralization in vitro. *Acta Biomater*. 2013;9:5771-9.
- [6] Kokubo T, Takadama H. How useful is SBF in predicting in vivo bone bioactivity? *Biomaterials*. 2006;27:2907-15.
- [7] Brauer DS, Mneimne M, Hill RG. Fluoride-containing bioactive glasses: Fluoride loss during melting and ion release in tris buffer solution. *J Non Cryst Solids*. 2011;357:3328-33.
- [8] Shah FA, Brauer DS, Wilson RM, Hill RG, Hing KA. Influence of cell culture medium composition on in vitro dissolution behavior of a fluoride-containing bioactive glass. *J Biomed Mater Res A*. 2014;102:647-54.
- [9] Martin RA, Twyman H, Qiu D, Knowles JC, Newport RJ. A study of the formation of amorphous calcium phosphate and hydroxyapatite on melt quenched Bioglass® using surface sensitive shallow angle X-ray diffraction. *J Mater Sci Mater Med*. 2009;20:883-8.
- [10] Hench LL, Andersson Ö. Bioactive Glasses. In: Hench LL, Wilson J, editors. *An Introduction to Bioceramics*. Singapore: World Scientific Publishing; 1993. p. 41-62.
- [11] Hench LL. The story of Bioglass®. *J Mater Sci Mater Med*. 2006;17:967-78.
- [12] Jones JR. Review of bioactive glass: From Hench to hybrids. *Acta Biomater*. 2012.
- [13] Bohner M, Lemaitre J. Can bioactivity be tested in vitro with SBF solution? *Biomaterials*. 2009;30:2175-9.
- [14] Webster TJ, Ergun C, Doremus RH, Siegel RW, Bizios R. Specific proteins mediate enhanced osteoblast adhesion on nanophase ceramics. *J Biomed Mater Res*. 2000;51:475-83.
- [15] Mahmood TA, Davies JE. Incorporation of amino acids within the surface reactive layers of bioactive glass in vitro: an XPS study. *J Mater Sci Mater Med*. 2000;11:19-23.
- [16] Kosoric J, Williams R, Hector M, Anderson P. A Synthetic Peptide Based on a Natural Salivary Protein Reduces Demineralisation in Model Systems for Dental Caries and Erosion. *Int J Pept Res Ther*. 2007;13:497-503.
- [17] Shah FA, Brauer DS, Desai N, Hill RG, Hing KA. Fluoride-containing bioactive glasses and Bioglass® 45S5 form apatite in low pH cell culture medium. *Mater Lett*. 2014;119:96-9.

- [18] Guth K, Campion C, Buckland T, Hing KA. Effects of serum protein on ionic exchange between culture medium and microporous hydroxyapatite and silicate-substituted hydroxyapatite. *J Mater Sci Mater Med*. 2011;22:2155-64.
- [19] Kim CY, Clark AE, Hench LL. Early stages of calcium-phosphate layer formation in bioglasses. *J Non Cryst Solids*. 1989;113:195-202.
- [20] Hill RG, Brauer DS. Predicting the bioactivity of glasses using the network connectivity or split network models. *J Non Cryst Solids*. 2011;357:3884-7.
- [21] Brauer DS, Karpukhina N, O'Donnell MD, Law RV, Hill RG. Fluoride-containing bioactive glasses: Effect of glass design and structure on degradation, pH and apatite formation in simulated body fluid. *Acta Biomater*. 2010;6:3275-82.
- [22] Müller L, Müller FA. Preparation of SBF with different HCO₃⁻ content and its influence on the composition of biomimetic apatites. *Acta Biomater*. 2006;2:181-9.
- [23] Wilson RM, Elliott JC, Dowker SE, Smith RI. Rietveld structure refinement of precipitated carbonate apatite using neutron diffraction data. *Biomaterials*. 2004;25:2205-13.

Figure Captions

Figure 1: Concentrations of Ca²⁺, P, and F⁻ in culture media (a-c) HC-, and (d-f) HS-MEM after immersion of BG. Insets: (d) Ca²⁺ and (e) P concentrations for F0 and 45S5 at day 7 (HS-MEM).

Figure 2: FTIR spectra of glasses after immersion for 3 days (grey) and 7 days (black) in (a) HC-MEM and (b) HS-MEM. Apatite formation, as interpreted from the appearance of split PO₄³⁻ (ν 4) peaks and broad sharp PO₄³⁻ (ν 3) absorption band, is severely delayed in HS-MEM (arrows).

Figure 3: XRD patterns of glasses after immersion for 3 days (grey) and 7 days (black) in (a) HC-MEM and (b) HS-MEM. Inset: Detailed view of F4 in HC-MEM at day 7 showing characteristic reflections for apatite in the 30-35° 2θ range.